

Non-reciprocal ultrafast laser writing

WEIJIA YANG¹, PETER G. KAZANSKY^{1*} AND YURI P. SVIRKO²

¹Optoelectronics Research Centre, University of Southampton SO17 1BJ, UK

²Department of Physics and Mathematics, University of Joensuu, FI-80101, Finland

*e-mail: pgk@orc.soton.ac.uk

Published online: 13 January 2008; doi:10.1038/nphoton.2007.276

Photosensitivity is a material property that is relevant to many phenomena and applications, from photosynthesis and photography to optical data storage and ultrafast laser writing. It was commonly thought that, in a homogeneous medium, photosensitivity and the corresponding light-induced material modifications do not change on reversing the direction of light propagation. Here we demonstrate that when the direction of the femtosecond laser beam is reversed from the $+z$ to $-z$ direction, the structures written in LiNbO_3 crystal when translating the beam along the $+y$ and $-y$ directions are mirrored. In a non-centrosymmetric medium, modification of the material can therefore differ for light propagating in opposite directions. This is the first evidence of a new optical phenomenon of non-reciprocal photosensitivity. We interpret this effect in terms of light pressure and associated heat flow, resulting in a temperature gradient in homogeneous media without inversion symmetry under uniform intense irradiation.

Modification of materials with ultrafast lasers^{1,2} has recently attracted considerable interest because of its relevance to a wide range of applications including laser surgery^{3,4}, integrated optics^{5–12}, optical data storage^{13,14} and three-dimensional micro-^{15–20} and nano-structuring^{21–27}. In particular, refractive-index changes^{28–31} and micro-explosion-induced voids³² have been demonstrated in LiNbO_3 crystal, which is an excellent material for electro-, acousto- and nonlinear optical applications^{33–37}. Recently, a remarkable quill writing effect manifesting itself as a strong dependence of the material modification on the writing direction has been discovered in silica glass, and has been explained by a tilt of the intensity front of an ultrashort pulse³⁸. Here we demonstrate, both experimentally and theoretically, that in a non-centrosymmetric crystal, modification of the material can differ when an untilted light beam moves in opposite directions within the crystal and, moreover, when light propagates in opposite directions. It was commonly thought that light-induced modifications and the related photosensitivity do not change on the reversal of the direction of light propagation in a homogeneous medium. Here we present the first evidence of non-reciprocal photosensitivity. We anticipate that this non-reciprocity of ultrafast laser writing will lead to new opportunities in material processing^{39,40}, optical manipulation⁴¹ and data storage⁴².

We wrote structures directly onto z -cut LiNbO_3 by translating along the y axis of the crystal a tightly focused ultrafast laser beam that propagates in the z axis. Surprisingly, we discovered that when the direction of light propagation was reversed from the $+z$ direction to the $-z$ direction, the structures written in the crystal when translating the beam along the $+y$ and $-y$ directions were mirrored. The phenomenon of laser writing in LiNbO_3 is therefore non-reciprocal; that is, a single light beam interacts with the crystal differently for opposite directions of light propagation. This experimental finding implies that forward- and backward-propagating intense light beams interact with the crystal differently, resembling the conventional Faraday

effect. Therefore laser writing in LiNbO_3 can be seen as a new non-reciprocal, nonlinear optical phenomenon.

RESULTS

STRUCTURES WRITTEN IN DIFFERENT DIRECTIONS

First, groups of lines with various pulse energies ranging from $1 \mu\text{J}$ to $2.4 \mu\text{J}$ were written below the $-z$ face of the LiNbO_3 sample (see Methods). The scan speed was $200 \mu\text{m s}^{-1}$ and the laser beam was linearly polarized along the y axis. For each group two lines were produced in opposite directions, in other words with the writing direction along the $-y$ and $+y$ axes of LiNbO_3 , respectively (Fig. 1). We observed different material modifications depending on the pulse energy and the writing direction. With pulses energies below $1.4 \mu\text{J}$, a positive phase change ($\Delta\varphi$) and thus a positive refractive index change (Δn) was created in the exposed region for the lines written in both directions (Fig. 1a). The lines had a width of $3 \mu\text{m}$, which is close to the focal spot size of the laser beam (Fig. 1a). No difference was observed between the lines written in the two directions. The lines imprinted with pulses energies between $1.4 \mu\text{J}$ and $2 \mu\text{J}$ still had a positive Δn in both directions (Fig. 1c). However, we observed the appearance of a directional dependence in the structures written along the $-y$ and $+y$ axes of LiNbO_3 . The difference was first revealed in the morphology of the line structures. The lines inscribed along the $-y$ axis of LiNbO_3 had a larger width than those along the $+y$ axis (Fig. 1c). In addition, the directional difference was also revealed from the $\Delta\varphi$ in the structures. The lines written along the $-y$ axis of LiNbO_3 produced a larger positive $\Delta\varphi$ than those along the $+y$ axis (Fig. 1e). With a further increase of the pulse energy above $2 \mu\text{J}$, this dependence could also be observed from the different textures of the lines written in opposite directions. Some optically damaged regions appeared in the lines written along the $+y$ axis of LiNbO_3 (Fig. 1d). In contrast, no damage could be observed in the entire line written along the $-y$ axis. The $\Delta\varphi$ profile of the lines is shown in Fig. 1f. The line

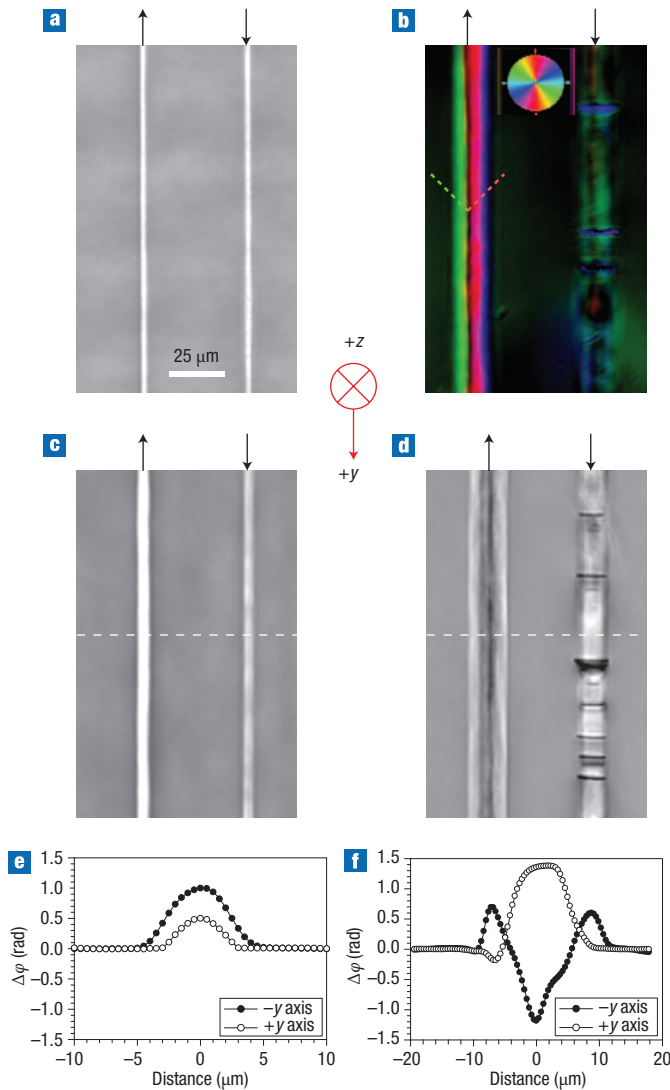


Figure 1 Line structures written along the y axis of the LiNbO_3 sample. **a–d**, Quantitative phase microscope images (grey) and quantitative birefringence image (coloured) of the lines written along the $-y$ axis (left lines in each image) and the $+y$ axis (right lines in each image) of LiNbO_3 with pulse energies of 1.2 μJ (a), 2.4 μJ (b), 1.8 μJ (c), 2.4 μJ (d). The brightness in **b** represents the retardance magnitude and the colour represents the slow axis of the birefringence region. The colour of the circular legend shows the direction of the slow axis. The dashed lines show the slow axis of the birefringence region. **e,f** Quantitative $\Delta\varphi$ profiles of the line structures written along the $-y$ and $+y$ axes at the dashed line in **c** (**e**) and **d** (**f**), respectively. Writing directions of the structures in **a–d** are shown by arrows and the lines were written by propagating the laser beam along the $+z$ axis.

inscribed along the $+y$ axis still had a positive $\Delta\varphi$, similar to those created with lower pulse energies, and exhibited a maximum $\Delta\varphi$ of 1.4 rad. By assuming the length of the structure along the z axis to be $\sim 30 \mu\text{m}$, the maximum Δn was 4×10^{-3} . However, the line written along the $-y$ axis exhibited a more complex $\Delta\varphi$ profile. A central dip region shows a negative $\Delta\varphi$, whereas the surrounding regions have a positive $\Delta\varphi$. This observation indicates that femtosecond laser modification results in a negative Δn of the central exposed region and a positive Δn of the surrounding region. Stressed regions created as a result of

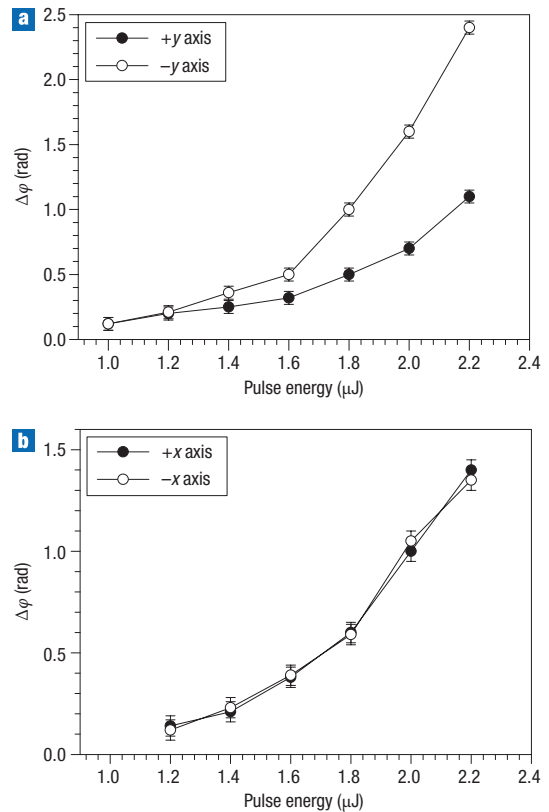


Figure 2 Comparison of the line structures imprinted along the y and x axes. **a,b**, Measured $\Delta\varphi$ of the line structures versus pulse energies for the lines written along the y axis of the LiNbO_3 sample (a) and the x axis of the LiNbO_3 sample (b). Error bars represent variations in the phase value for the unexposed region of the LiNbO_3 sample.

the expansion of the material at the focus of the writing laser beam can account for the positive Δn of the surrounding region^{27–29}. This was confirmed by quantitative birefringence imaging of the line structures (Fig. 1b). The line created along the $-y$ axis of the sample shows two birefringent regions surrounding the central irradiated region, and the slow axis of the birefringent region is inclined at $\sim 45^\circ$ towards the writing direction. The amorphization of the focal volume and subsequent stress-induced birefringence could account for this type of modification. In contrast, no birefringence features could be observed in the structures written along the $+y$ axis. It can also be noted that the birefringence becomes weaker when the pulse energy decreases, and no birefringence could be observed when the pulse energy was below 2 μJ . Moreover, the directional dependence does not depend on the laser polarization. Compared with the structures imprinted when the crystal was translated along the y axis, no directional dependence was observed when the structures were written by translating the crystal along the x axis (Fig. 2). This indicates that the directional dependence of the light-induced modifications in LiNbO_3 is associated with the crystal symmetry.

THE DEPENDENCE OF WRITING ON THE CRYSTAL AXIS ORIENTATION

To verify that the directional dependence of the modifications along the y axis of LiNbO_3 was defined by the crystal axes, four groups of lines were fabricated in the sample. Two groups of

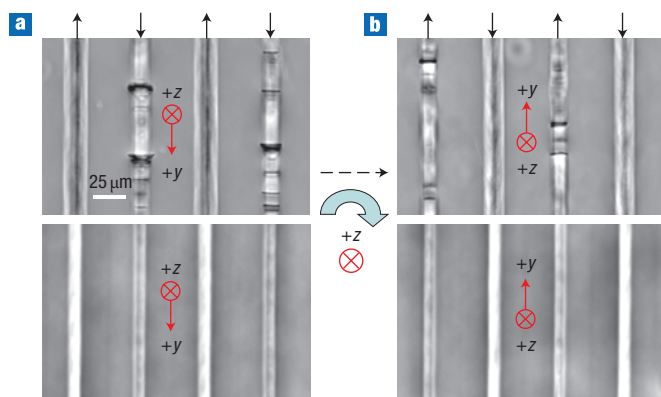


Figure 3 Phase images of line structures in the rotation experiment. **a,b**, Quantitative phase microscope images of lines imprinted along the y axis with $2.4 \mu\text{J}$ (top) and $2 \mu\text{J}$ (bottom) pulse energies. The lines were written before (a) and after (b) rotating by 180° around the z axis of the crystal.

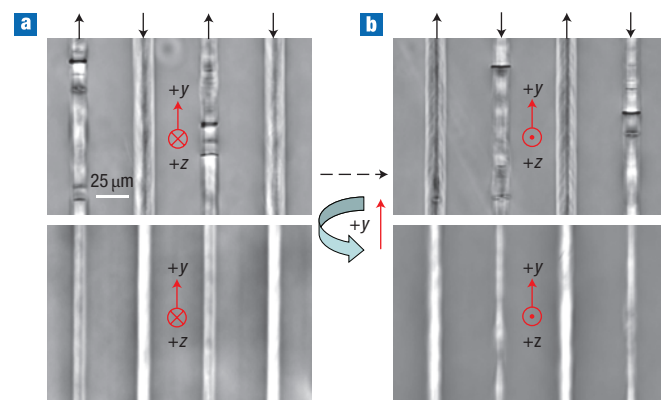


Figure 4 Phase images of line structures in the flip experiment. **a,b**, Quantitative phase microscope images of lines written along the y axis with $2.4 \mu\text{J}$ (top) and $2 \mu\text{J}$ (bottom) pulse energies. The lines were written by propagating the laser beam along the $+z$ axis (a) and the $-z$ axis (b) of the crystal, respectively.

lines with opposite writing directions, along the $-y$ and $+y$ axis respectively, were written inside the sample with pulse energies of $2.4 \mu\text{J}$ and $2 \mu\text{J}$. (Fig. 3a). The sample was then rotated by 180° around the z axis, and another two groups of structures, with the same writing parameters (including the direction of the stage movement), were then imprinted in the sample (Fig. 3b). By comparing Fig. 3a and b one can observe that the modification of the crystal structure is determined by the orientation of the writing direction with respect to the y axis of the crystal.

WRITING WITH A REVERSED LASER BEAM

Groups of structures were then written by the laser beam propagating along the $+z$ (Fig. 4a) and the $-z$ (Fig. 4b) axes of the crystal. As expected, the created structures were different for writing directions along the $+y$ and $-y$ axes of the sample. However, we were surprised to observe a mirror change in the structural modifications when the propagation direction of the writing beam was reversed. Indeed, in contrast to the lines

written along the $+y$ axis with $2.4 \mu\text{J}$ pulse energy by the beam propagating along the $+z$ axis, which showed optical damage features (Fig. 4a), no damage could be observed in the lines imprinted with the same fabrication parameters by the beam propagating along $-z$ axis (Fig. 4b). The change in structural modifications between these lines was only produced by reversing the propagation direction of the focused laser beam with respect to the z axis of the crystal. Moreover, the modification features, which appeared previously in the line written along the $+y$ axis by focusing below the $-z$ face of the crystal, could only be observed in the line written along the $-y$ axis when focusing below the $+z$ face. A mirror change of the modifications in two similar structures written along the y axis ($+y$ and $-y$ directions) with the reversal of the beam propagation direction along the z axis was therefore discovered. A similar mirror change of phase profiles, was also observed for the line structures, without strong damage features, when written with a pulse energy of $2 \mu\text{J}$.

We also used different writing speeds and observed that the linewidth increases when the scan speed is reduced. This indicates that a heat accumulation effect takes place during the writing process.

PICOSECOND LASER EXPERIMENT

Groups of line structures were also written in a z -cut LiNbO_3 sample using a picosecond laser system (Lumera Super Rapid), operating at $1,064 \text{ nm}$ with 9 ps pulse duration, 250 kHz repetition rate, and with pulse energies comparable to those used with the femtosecond laser system. Modifications with crack features were observed at the same fluencies and at intensities of about one order of magnitude lower compared with the femtosecond laser system, and with no evidence of the non-reciprocal writing phenomenon. This indicates that ultrashort pulses are necessary for the creation of the phenomenon, possibly because of the higher intensities that can be achieved with femtosecond pulses without strong damage to the sample.

LITHIUM NIOBATE CRYSTAL VERSUS SILICA GLASS

It should be noted that the asymmetry of writing in opposite directions (the femtosecond-laser quill writing effect) has been observed in silica glass³⁸. However, the directional asymmetry of ultrashort-pulse light-induced modifications in glass does not depend on the orientation of the medium or the direction of light propagation and can be controlled by the tilt of a pulse front. It has been suggested that the ponderomotive force (light pressure) at the front of the pulse is responsible for the phenomenon. The light pressure produced by the tilted front of the pulse can drag electrons from the electron plasma (generated as a result of multiphoton absorption) in the direction of the writing light-beam movement, in a kind of ‘snowplough’ effect.

However, in contrast to glass, the directional dependence of writing in LiNbO_3 depends on the orientation of the crystal with respect to the direction of the beam movement and the direction of light propagation. Specifically, the created structures have a strong anisotropy only when the focused beam is translated along the y axis, and no anisotropy is observed when the beam is translated along the x axis. The mirror symmetry of the structures created by the light beam propagating along the $+z$ and $-z$ axes of the crystal (see Fig. 4) indicates that the phenomenon observed in LiNbO_3 is not related to the tilt of the pulse front, as is the case for the femtosecond-laser quill writing effect in glass. We show in the following that, in a crystalline medium, even the pressure produced by a non-tilted pulse front can result in a dependence of the created structures on both the direction of writing and the propagation direction of the laser beam.

MECHANISM OF THE PHENOMENON

A heat current \mathbf{J} , which is carried by the electrons of the plasma created by the femtosecond laser pulse, and generated by the ponderomotive force and the photon drag effect, can be phenomenologically presented in the following form:

$$J_i = \eta_{ijklmn} E_j E_k^* \nabla_n (E_l E_m^*) + i \zeta_{ijklmn} E_j E_k E_l^* E_m^* k_n \quad (1)$$

where subscripts denote cartesian indices and \mathbf{E} is the complex amplitude of the light electric field; that is, $E_k E_l^*$ is proportional to the light intensity and is responsible for heating through plasma absorption. The first and second terms on the right-hand side of equation (1) describe pressure created by the front of the pulse and the photon drag effect⁴⁴, respectively; η_{ijklmn} and $\zeta_{ijklmn} = \zeta_{ikjlmn} = \zeta_{ilmjkn}$ are sixth rank tensors describing the material asymmetry; and \mathbf{k} is the wavevector. When the light beam propagates along the z axis of the LiNbO₃ crystal, the current along the x axis is identically zero by symmetry, and that along the y axis comprises symmetry allowed components of tensors η_{ijklmn} and ζ_{ijklmn} . For example, for the y -polarized light beam, the thermal current along the y axis given by

$$J_y = \left(\eta_{yyyyyz} \frac{\partial |E_y|^2}{\partial z} + ik \zeta_{yyyyyz} |E_y|^2 \right) |E_y|^2. \quad (2)$$

We will refer to this phenomenon as the photothermal effect in non-centrosymmetric media, or the bulk photothermal effect, to highlight that the light-induced heat current can be excited even under homogeneous illumination and in a homogeneous non-centrosymmetric medium⁴⁵.

However, the developed phenomenological description of the observed effect does not explain why the heat current produced by the laser beam can manifest itself in the modification of a moving sample. The major difficulty here is that the timescales of these processes are very different. Specifically, the laser field, which drives the heat current, as described by equation (1), is around for only ~ 150 fs. The created electrons in the laser-produced plasma thermally equalize with the lattice in a few picoseconds and finally recombine with nearby ions in just a few nanoseconds or even faster. However, at the pulse repetition rate of 250 kHz, the time interval between laser pulses is at least 1,000 times longer. What is there that ‘remembers’ what direction the laser beam is being translated in $4 \mu\text{s}$ later, when the next laser pulse arrives?

The short answer is that anisotropic energy distribution created by the short lasting current described by equation (1) is finally imprinted in the anisotropy of lattice temperature across the irradiated area. This can be seen as more efficient heating of the material when subsequent pulses arrive in a region to where the electric-field-driven heat current has already pushed thermal energy from another part of the beam owing to the crystal anisotropy. To clarify this, recall that our experiments were performed in the so-called thermal accumulation regime⁴⁶. In this regime, the material temperature is determined by the cumulative effect of many laser pulses. This is because, in our experimental conditions (beam diameter $d = 2 \mu\text{m}$, thermal diffusivity $D = \kappa/\rho c_p \approx 10^{-2} \text{ cm}^2 \text{ s}^{-1}$, thermal conductivity $\kappa \approx 2 \text{ W mK}^{-1}$, specific heat capacity $c_p \approx 714 \text{ J kg}^{-1} \text{ K}^{-1}$, volume mass density $\rho \approx 4,640 \text{ kg m}^{-3}$, pulse repetition rate $f = 250 \text{ kHz}$, sample velocity $v = 200 \mu\text{m s}^{-1}$), the effective cooling time $\tau_c = d^2/D \approx 4 \mu\text{s}$ coincides with $1/f$ and the thermal diffusion length $L_D = (4D/f)^{1/2} \approx 4 \mu\text{m}$ is comparable with the beam diameter. The distance travelled by the sample between two

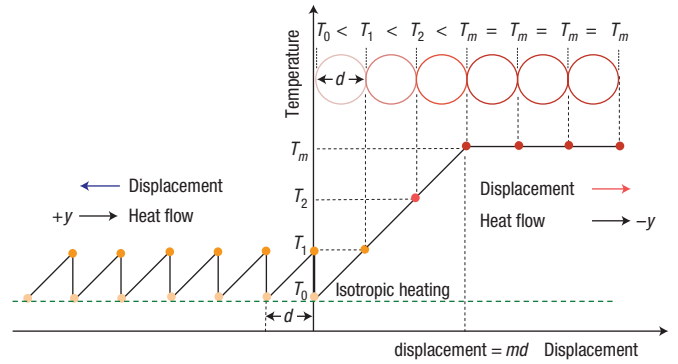


Figure 5 Illustration of the differential heating of a crystal as a result of the bulk photothermal effect. Heat flows (black arrow) in the $-y$ direction of the crystal. The temperature of the crystal increases until saturation when the beam is displaced in the direction of heat flow (red arrow) and oscillates near the level defined by isotropic heating (green dashed line) when displacement is opposite to the heat flow (blue arrow). The large circles illustrate the laser beam and increasingly darker colour corresponds to increasing temperature of the sample in the position of the beam.

consecutive pulses is $h = v/f = 0.8 \text{ nm}$; that is, the number of laser pulses overlapping within the beam diameter is $N = d/h = 2,500$. Such a small beam shift between two pulses implies that the beam movement can be considered to be continuous.

The absorption of the laser radiation results in an average heat production within the focus area with a rate

$$\left(\frac{\partial Q}{\partial t} \right)_{\text{homogeneous}} = a(\tau_p \times f)I, \quad (3)$$

where I is the laser intensity, τ_p is the pulse duration, and a is determined by the absorption coefficient, the volume of the irradiated area and so on. This heating homogeneously increases the temperature within the whole focal area. However, in the LiNbO₃ focal area there exists an average heat current along the y axis (equation (1)) of

$$\bar{J}_y = b(\tau_p \times f)I^2 \quad (4)$$

where b is determined by relevant non-zero components of the material tensors introduced in equation (1). When the light beam is propagated along the z axis of the crystal, this flow will push the heat along the y axis at the transfer rate

$$\left(\frac{\partial Q}{\partial t} \right)_{\text{anisotropic}} = A\bar{J}_y, \quad (5)$$

where A is the cross-section of the irradiated area in the XZ plane. This heat transfer will produce a temperature difference between opposite sides of the beam of

$$\Delta T = \frac{d}{\kappa A} \left(\frac{\partial Q}{\partial t} \right)_{\text{anisotropic}} = \frac{d}{\kappa} \bar{J}_y. \quad (6)$$

The sign of ΔT depends on the parameter b , that is, on the relevant component of the material tensor responsible for the observed effect. In particular, if the laser beam is y -polarized and

$\text{Im}\{\zeta_{yyyyz}\} > 0$, then $J_y < 0$. Therefore, if the y axis is horizontal with negative direction to the right, the temperature of the right-hand side of the irradiated area will be higher than that of the left-hand side (Fig. 5). In such a case the direction of the beam movement along the y axis does matter. Specifically, the temperature of the crystal when the beam is translated along the y axis in the negative direction will always be higher than that when the beam is translated along the y axis in the positive direction.

The mechanism of this direction-dependent writing can be visualized using the simplified model presented in Fig. 5. In this model, for the sake of simplicity, the beam movement is assumed to be discontinuous; that is, the beam movement along the y axis consists of jumps equal to the beam diameter in length. The conventional absorption described by equation (3) produces homogeneous heating of the irradiated area at temperature T_0 . If no other heating mechanisms are present, the temperature is the same for any position of the beam and does not depend on the direction in which the beam is moved. However, if the anisotropic heating mechanism described by equation (4) is involved, the temperature at the right side of the beam is higher than that of the left side by $\Delta T = dJ_y/\kappa$. When the beam jumps to the right (to the negative direction of the y axis) to its next placement, the temperature of the left side of the beam increases to $T + \Delta T$, and the temperature of the right side of the beam is T . The anisotropic heating mechanism is switched on and increases the temperature of the right side so that it will be ΔT higher than that of the left side of the beam. As a result, the temperature of the right side of the beam will be equal to $T + 2\Delta T$. The same temperature increase will happen after the next jump. After m jumps in the direction that coincides with the direction of the anisotropic heat flow, the temperature of the rightmost irradiated area will be equal to

$$T_{\text{parallel}}^{\text{max}} = T_0 + \frac{md}{\kappa} \times \bar{J}_y. \quad (7)$$

When the light beam moves in the positive direction along the y axis, the temperature of the left side of the beam is the same after each jump. Therefore, although the anisotropic heating mechanism results in an increase of the temperature of the right side of the beam, the temperature of the crystal does not increase (Fig. 5):

$$T_{\text{opposite}}^{\text{max}} = T_0 + \frac{d}{\kappa} \times \bar{J}_y. \quad (8)$$

So, the anisotropic heating may result in a very different scenario for the laser writing, which we refer to as differential heating of the sample. This increase of the temperature described by equation (7) will eventually slow down owing to thermal diffusion and melting of the sample. Moreover uneven heating of the sample when the beam moves opposite to the heat flow, which is described by equation (8) and illustrated in Fig. 5, may result in shock-induced damage, which is evident for one of the writing directions (Figs 3 and 4). In real experimental conditions, the situation is apparently more complicated, because we need to account for the interplay of thermal diffusion and accumulation; however, the simplified model above illustrates well how anisotropic heating can manifest itself in crystal modification by a moving laser beam.

DISCUSSION

The restrictions imposed on the light-induced current by crystalline symmetry explain the observed directional dependence of writing. Specifically, because the light beam propagating along the z axis does not produce thermal current along the x axis, the crystal modification is not sensitive to the translation of the light beam along the x axis. However, when the beam is translated along the y axis, the in-plane heat flow is either parallel or antiparallel to the beam velocity. Because the heating of the crystal is stronger when the direction of the heat flow coincides with the direction of the beam movement, modification of the non-centrosymmetric crystal shows a pronounced directional dependence independent of the tilt of the pulse front. It should also be noted that we observed similar crystal modifications for the x - and y -polarized beams. Such an experimental finding is also supported by crystal symmetry because in the LiNbO_3 crystal, the thermal current along the y axis is not forbidden for x - or y -polarized beams; however, the current is described by different independent components of the material tensor. The similarity in the crystal modifications produced with the x - and y -polarized beams indicates that these components are of the same order of magnitude.

From equations (1) and (2) it can be observed that the interplay of the crystal anisotropy and light-induced heat flow gives rise to a new non-reciprocal, nonlinear optical phenomenon—non-reciprocal photosensitivity. In the LiNbO_3 , the non-reciprocal photosensitivity manifests itself as a change in the sign of the light-induced current when the light propagation direction is reversed. This phenomenon is visualized when modification of the crystal is performed by a moving light beam; in such a case the created pattern is mirrored when the light propagation direction is reversed.

In conclusion, we report the first realization of non-reciprocal ultrafast laser writing in z -cut LiNbO_3 crystal by a tightly focused ultrafast laser beam. We discovered that when the direction of the laser beam is reversed from the $+z$ direction to the $-z$ direction, the structures written in the crystal when translating the beam along the $+y$ and $-y$ directions are mirrored. Therefore, a single light beam interacts with the crystal differently for opposite directions of light propagation. This new non-reciprocal, nonlinear optical phenomenon is interpreted in terms of light pressure at the front of an ultrashort pulse, photon drag effect and the associated light-induced thermal current in crystalline media. We would like to point out that non-reciprocal phenomena are very rare in optics and are usually associated with the breaking of time-reversal symmetry owing to the presence of a magnetic field. Examples include the conventional Faraday effect and magneto-chiral dichroism⁴⁷, when interaction of a single light beam with a homogeneous material is different for two opposite directions, similarly to the non-reciprocal photosensitivity reported here.

METHODS

LASER WRITING

The experiments were performed using a mode-locked, regeneratively amplified Ti:sapphire laser system (Coherent RegA 9000), operating at 800 nm with 150 fs pulse duration and 250 kHz repetition rate. The linearly polarized laser beam was focused using a $\times 50$ objective (numerical aperture, $\text{NA} = 0.55$), 150 μm below the surface of a 1-mm-thick LiNbO_3 sample. The spot size in the focus of the beam was estimated to be $\sim 2 \mu\text{m}$. Laser polarization was controlled using a half-wave plate, and the pulse energy was varied using a neutral density filter. The sample was mounted on a computer-controlled linear motorized stage (Aerotech ALS-130). Straight lines of modifications were written by translating the sample

perpendicular to the propagation direction of the laser beam. The writing direction was defined as the scan direction of the laser spot with respect to the LiNbO₃ sample.

CHARACTERIZATION OF THE STRUCTURES

After irradiation, the structural modifications were inspected by quantitative phase microscopy⁴³ (QPM), using an Olympus BX51 optical microscope equipped with a motorized focusing stage (Physik Instrumente). A quantitative phase map of the structures was produced using the QPM software (Iatia Vision Sciences). The refractive-index change of the structure was estimated from $\Delta n = \Delta\varphi\lambda/(2\pi w)$, where $\Delta\varphi$ is the phase shift of the light at wavelength 550 nm and w is the thickness of the structure along the light propagation direction. The stress region was analysed using a quantitative birefringence imaging system (CRi Abrio Imaging System).

Received 2 August 2007; accepted 28 November 2007;
published 13 January 2008

References

1. Stuart, B. C., Feit, M. D., Rubenchik, A. M., Shore, B. W. & Perry, M. D. Laser-induced damage in dielectrics with nanosecond to subpicosecond pulses. *Phys. Rev. Lett.* **74**, 2248–2251 (1995).
2. Tien, A. C., Backus, S., Kapteyn, H., Murmane, M. & Mourou, G. Short-pulse laser damage in transparent materials as a function of pulse duration. *Phys. Rev. Lett.* **82**, 3883–3886 (1999).
3. Birngruber, R. *et al.* Femtosecond laser tissue interactions—retinal injury studies. *IEEE J. Quant. Electron.* **23**, 1836–1844 (1987).
4. Tirlapur, U. K. & Konig, K. Cell biology-targeted transfection by femtosecond laser. *Nature* **418**, 290–291 (2002).
5. Davis, K. M., Miura, K., Sugimoto, N. & Hirao, K. Writing waveguides in glass with a femtosecond laser. *Opt. Lett.* **21**, 1729–1731 (1996).
6. Streltsov, A. M. & Borrelli, N. F. Fabrication and analysis of a directional coupler written in glass by nanosecond femtosecond laser pulses. *Opt. Lett.* **26**, 42–43 (2001).
7. Osellame, R. *et al.* Femtosecond writing of active optical waveguides with astigmatically shaped beams. *J. Opt. Soc. Am. B* **20**, 1559–1567 (2003).
8. Watanabe, W., Asano, T., Yamada, K., Itoh, K. & Nishii, J. Wavelength division with three-dimensional couplers fabricated by filamentation of femtosecond laser pulses. *Opt. Lett.* **28**, 2491–2493 (2003).
9. Chan, J. W., Huser, T. R., Risbud, S. H. & Krol, D. M. Modification of the fused silica glass network associated with waveguide fabrication using femtosecond laser pulses. *Appl. Phys. A* **76**, 367–372 (2003).
10. Eaton, S. M., Zhang, H. B. & Herman, P. R. Heat accumulation effects in femtosecond laser-written waveguides with variable repetition rate. *Opt. Express* **13**, 4708–4716 (2005).
11. Okhrimchuk, A. G., Shestakov, A. V., Khrushchev, I. & Mitchell, J. Depressed cladding, buried waveguide laser formed in a YAG:Nd³⁺ crystal by femtosecond laser writing. *Opt. Lett.* **30**, 2248–2250 (2005).
12. Graf, R. *et al.* Pearl-chain waveguides written at megahertz repetition rate. *Appl. Phys. B* **87**, 21–27 (2007).
13. Glezer, E. N. *et al.* Three-dimensional optical storage inside transparent materials. *Opt. Lett.* **21**, 2023–2025 (1996).
14. Kawamura, K., Hirano, M., Kamiya, T. & Hosono, H. Holographic writing of volume-type microgratings in silica glass by a single chirped laser pulse. *Appl. Phys. Lett.* **81**, 1137–1139 (2002).
15. Ashkenasi, D. *et al.* Fundamentals and advantages of ultrafast micro-structuring of transparent materials. *Appl. Phys. A* **77**, 223–228 (2003).
16. Glezer, E. N. & Mazur, E. Ultrafast-laser driven micro-explosions in transparent materials. *Appl. Phys. Lett.* **71**, 882–884 (1997).
17. Seet, K. K., Mizekic, V., Matsuo, S., Juodkazis, S. & Misawa, H. Three-dimensional spiral-architecture photonic crystals obtained by direct laser writing. *Adv. Mater.* **17**, 541–545 (2005).
18. Pommellec, B., Sudrie, L., Franco, M., Prade, B. & Mysyrowicz, A. Femtosecond laser irradiation stress induced in pure silica. *Opt. Express* **11**, 1070–1079 (2003).
19. Sudrie, L. *et al.* Femtosecond laser-induced damage and filamentary propagation in fused silica. *Phys. Rev. Lett.* **89**, 186601 (2002).
20. Marshall, G. D., Ams, M. & Withford, M. J. Direct laser written waveguide-Bragg gratings in bulk fused silica. *Opt. Lett.* **31**, 2690–2691 (2006).
21. Kazansky, P. G. *et al.* Anomalous anisotropic light scattering in Ge-doped silica glass. *Phys. Rev. Lett.* **82**, 2199–2202 (1999).
22. Shimotsuma, Y., Kazansky, P. G., Qiu, J. R. & Hirao, K. Self-organized nanogratings in glass irradiated by ultrashort light pulses. *Phys. Rev. Lett.* **91**, 247705 (2003).
23. Hnatovsky, C. *et al.* Polarization-selective etching in femtosecond laser-assisted microfluidic channel fabrication in fused silica. *Opt. Lett.* **30**, 1867–1869 (2005).
24. Yang, W. J., Bricchi, E., Kazansky, P. G., Bovatsek, J. & Arai, A. Y. Self-assembled periodic sub-wavelength structures by femtosecond laser direct writing. *Opt. Express* **14**, 10117–10124 (2006).
25. Qiu, J. R. *et al.* Manipulation of gold nanoparticles inside transparent materials. *Angew. Chem. Int. Edn* **43**, 2230–2234 (2004).
26. Dubov, M., Mezentssev, V., Bennion, I. & Nikogosyan, D. N. UV femtosecond laser inscribes a 300 nm period nanostructure in a pure fused silica. *Meas. Sci. Technol.* **18**, 15–17 (2007).
27. Podlipensky, A., Abdolvand, A., Seifert, G. & Graener, H. Femtosecond laser assisted production of dichroitic 3D structures in composite glass containing Ag nanoparticles. *Appl. Phys. A* **80**, 1647–1652 (2005).
28. Gui, L., Xu, B. X. & Chong, T. C. Microstructure in lithium niobate by use of focused femtosecond laser pulses. *IEEE Photon. Technol. Lett.* **16**, 1337–1339 (2004).
29. Thomson, R. R., Campbell, S., Blewett, I. J., Kar, A. K. & Reid, D. T. Optical waveguide fabrication in z-cut lithium niobate (LiNbO₃) using femtosecond pulses in the low repetition rate regime. *Appl. Phys. Lett.* **88**, 111109 (2006).
30. Burghoff, J., Hartung, H., Nolte, S. & Tunnermann, A. Structural properties of femtosecond laser-induced modifications in LiNbO₃. *Appl. Phys. A* **86**, 165–170 (2007).
31. Burghoff, J., Grebing, C., Nolte, S. & Tunnermann, A. Waveguides in lithium niobate fabricated by focused ultrashort laser pulses. *Appl. Surf. Sci.* **253**, 7899–7902 (2007).
32. Zhou, G. Y. & Gu, M. Anisotropic properties of ultrafast laser-driven microexplosions in lithium niobate crystal. *Appl. Phys. Lett.* **87**, 241107 (2005).
33. Prokhorov, A. M. & Kuzminov, Y. S. *Physics and Chemistry of Crystalline Lithium Niobate* (Hilger, New York, 1990).
34. Weis, R. S. & Gaylor, T. K. Lithium niobate—summary of physical properties and crystal structure. *Appl. Phys. A* **37**, 191–203 (1985).
35. Glass, A. M., Linde, D. V. D. & Negran, T. J. High-voltage bulk photovoltaic effect and photorefractive process in LiNbO₃. *Appl. Phys. Lett.* **25**, 233–235 (1974).
36. Gallo, K., Assanto, G., Parameswaran, K. R. & Fejer, M. M. All-optical diode in a periodically poled lithium niobate waveguide. *Appl. Phys. Lett.* **79**, 314–316 (2001).
37. Shur, V. Y. *et al.* Nanoscale backswitched domain patterning in lithium niobate. *Appl. Phys. Lett.* **76**, 143–145 (2000).
38. Kazansky, P. G. *et al.* 'Quill' writing with ultrashort light pulses in transparent materials. *Appl. Phys. Lett.* **90**, 151120 (2007).
39. Chrisey, D. B. Materials processing—the power of direct writing. *Science* **289**, 879–881 (2000).
40. Livingston, F. E. & Helvajian, H. The symbiosis of light and matter: Laser-engineered materials for photo-functionality. *MRS Bull.* **32**, 40–46 (2007).
41. Garcés-Chávez, V., McGloin, D., Melville, H., Sibbett, W. & Dholakia, K. Simultaneous micromanipulation in multiple planes using a self-reconstructing light beam. *Nature* **419**, 145–147 (2002).
42. Juodkazis, S. *et al.* Three-dimensional recording by tightly focused femtosecond pulses in LiNbO₃. *Appl. Phys. Lett.* **89**, 062903 (2006).
43. Barty, A., Nugent, K. A., Paganin, D. & Roberts, A. Quantitative optical phase microscopy. *Opt. Lett.* **23**, 817–819 (1998).
44. Sturman, B. & Fridkin, V. M. *The Photovoltaic and Photorefractive Effects in Noncentrosymmetric Materials* (Gordon & Breach, New York, 1992).
45. Ivchenko, E. L. & Pikus, G. E. *Superlattices and Other Heterostructures: Symmetry and Optical Phenomena* (Springer, Berlin, 1995).
46. Nejadmalayeri, A. H. & Herman, P. R. Rapid thermal annealing in high repetition rate ultrafast laser waveguide writing in lithium niobate. *Opt. Express* **15**, 10842–10854 (2007).
47. Rikken, G. J. A. & Raupach, E. Observation of magneto-chiral dichroism. *Nature* **390**, 493–494 (1997).

Acknowledgements

The authors are grateful to K. Gallo and V.Y. Shur for helpful discussions and C. Corbari for help with the experiments. The work was supported by the Engineering and Physical Sciences Research Council (EPSRC). Y.P.S. would like to acknowledge the support of Academy of Finland (grant no. 115781) and the National Technology Agency of Finland (TEKES) (grant no. 40310). Correspondence and requests for materials should be addressed to P.G.K.

Reprints and permission information is available online at <http://npg.nature.com/reprintsandpermissions/>